

Article

Regional Correlation between Precipitation and Vegetation in the Huang-Huai-Hai River Basin, China

Denghua Yan ¹, Ting Xu ^{1,*} , Abel Girma ², Zhe Yuan ^{1,3}, Baisha Weng ¹, Tianling Qin ¹, Pierre Do ⁴ and Yong Yuan ^{1,5}

¹ State Key Laboratory of Simulation and Regulation of Water Cycle in River Basin, China Institute of Water Resources and Hydropower Research, Beijing 100038, China; yandh@iwhr.com (D.Y.); yuanzhe_0116@126.com (Z.Y.); baishaweng@126.com (B.W.); tianling406@163.com (T.Q.); yuanyong365@126.com (Y.Y.)

² College of Environmental Science and Engineering, Donghua University, Shanghai 201620, China; abelethiopia@yahoo.com

³ Changjiang River Scientific Research Institute, Wuhan 430010, China

⁴ Institute of Water Resources and Hydrology, Department of Hydraulic Engineering, Tsinghua University, Beijing 100084, China; dodmp10@mails.tsinghua.edu.cn

⁵ General Institute of Water Resources and Hydropower Planning and Design Ministry of Water Resources, Beijing 100120, China

* Correspondence: xuting900515@163.com

Received: 16 June 2017; Accepted: 21 July 2017; Published: 25 July 2017

Abstract: In a context of climate change, precipitation patterns show substantial disturbances and the occurrence of precipitation anomalies has tended to increase in the Huang-Huai-Hai River Basin. These anomalies are likely influencing vegetation dynamics and ecosystem stability. This paper aims to have a comprehensive understanding of vegetation growth response towards the precipitation pattern in the Huang-Huai-Hai River Basin. The study used NDVI (Normalized Difference Vegetation Index) data and mapped precipitation datasets from 1982 to 2011. NDVI and precipitation show a similar spatial distribution: they decrease from the southeast coast to the northwest inland. Regions with sparse vegetation are mainly distributed in arid and semi-arid areas or densely-populated areas. Vegetation coverage and the regular precipitation pattern show a positive correlation (61.6% of the whole region), while the correlation between vegetation coverage and precipitation anomalies is negative (62.7% for rainless days and 60.3% for rainstorm days). The clustering result shows that abundant vegetation is mainly situated in high precipitation or low anomaly areas. On the contrary, the degraded regions are mainly distributed in low precipitation or high anomaly areas. However, some special regions, mainly located in the Three North Shelterbelt Program region, the Tibetan Plateau, and other regions along the rivers, present improved vegetation cover when precipitation decreases or extreme events occur.

Keywords: NDVI; vegetation coverage; growing season precipitation; Huang-Huai-Hai river basin

1. Introduction

Vegetation, one of the ecological system roots, connects the atmosphere, soil, and water. Vegetation plays a significant role in soil and water conservation, climate regulation, and ecosystem stability, as well as the global ecological system [1]. To understand the vegetation dynamic changes on the world is necessary. Remote sensing observations, the most effective method to obtain large-area vegetation cover data, has been widely used, such as, Myneni et al. have used it to explore the plant growth in the Northern High Latitudes [2]. Liu et al. have used multi-temporal remote sensing image to analysis the landscape spatial patterns in east part of Beijing [3]. Karlson et al. have investigated

how the hands-on application of RS for vegetation analysis has developed in the Sudano-Sahelian zone by reviewing the scientific literature published between 1975 and 2014 [4]. Feng et al. have used AVHRR NDVI and in situ green biomass data to evaluate vegetation optical depth in West African Sahel [5]. GIMMS (Global Inventory Modelling and Mapping Studies) NDVI is able to take various factors of influence into account and with high accuracy [6]. This dataset is considered to be the best available for long-term greenery monitoring analysis [7,8]. The long-term NDVI time series data are a comprehensive method to understand large-area plant activities.

Spatio-temporal variations of large-area foliage cover are the combined result of climate change and human activities. These subjects are considered as popular research topics given the current global change [9–11]. However, for long periods, climate change should have the most influence on vegetation growth and distribution [12]. The main climatic factors include precipitation, temperature, solar exposure, and so on, among which precipitation is the major factor [13]. Spano et al. found that precipitation directly influences plant growth: foliage cover area was affected by precipitation variations [14]. Li et al. discovered in Senegal forests in that there was a positive correlation between NDVI and precipitation in dense greenery areas, and a negative one in sparse vegetation areas [15]. Wessels et al., Li et al., and Buyantuyev et al. all found that the large inter-annual variations of precipitation in amount and distribution would bring about large inter-annual variations and intra-annual dynamics of vegetation growth [16–18]. The influence of precipitation on vegetation growth is, therefore, evident, especially the impact from precipitation anomalies; the occurrence of precipitation anomalies influences the vegetation growth and the related ecosystem services [19].

In recent years, due to the influence of temporal and spatial precipitation patterns, the vegetation cover has changed, especially in the Huang-Huai-Hai River Basin. Its ecosystem stability plays a main role in China. However, because of the increasing precipitation anomalies, the vegetation cover has been disturbed and has caused a series of environmental disasters, such as water and soil erosion, and desertification [20]. The vegetation degradation seriously threatens the normal ecosystem cycle and has caused serious losses to agriculture and industry [21,22]. Consequently, exploring the vegetation processes to precipitation variability is essential. Which changes has vegetation coverage faced? How can these variations be correlated to spatio-temporal patterns of precipitation? Many scholars have conducted research on these issues for different parts of the basin, such as, Sun et al. have explore the relationship between fractional vegetation cover change and rainfall in the Yellow River Basin [23]. Jing et al. have conducted a study on the relationship between dynamic change of vegetation coverage and precipitation in Beijing's mountainous areas [24]. Zhao et al. have analyzed the driving forces of vegetation coverage change in the Loess Plateau [25]. Pang et al. have used the NDVI to identify variations of vegetation to climate change on the Tibetan Plateau [26]. However, few researchers have investigated the whole basin, and even fewer have considered the impact of precipitation anomalies on vegetation. The vegetation sensitivity to precipitation, precipitation anomaly variations, and the corresponding spatio-temporal reaction patterns in the whole basin are not yet thoroughly understood. A better understanding of these issues could enrich our knowledge on ecosystem resilience to precipitation variability. Additionally, this would be a good opportunity to identify the areas particularly prone to precipitation anomalies and provide useful data for hazard prediction.

The main objectives were to: (1) analyze the spatio-temporal variations of the precipitation and precipitation anomalies; (2) analyze the spatio-temporal variations of the vegetation coverage and their regularity in the basin; and (3) investigate the influence of the precipitation and precipitation anomalies on the vegetation coverage. In this way, the study intends to understand the potential influences of increased precipitation variability on ecosystems of the Huang-Huai-Hai River Basin.

2. Materials and Methods

2.1. Study Site

The Huang-Huai-Hai River Basin is located at $95^{\circ} 53' - 122^{\circ} 60' E$, $32^{\circ} 10' - 43^{\circ} N$ between several remarkable geological formations, such as the Tibetan Plateau, Inner Mongolia Plateau, Loess Plateau, and Huang-Huai-Hai Plain, from west to east. The basin area is about 1,445,000 km² covering 14 provinces, including Qinghai, Sichuan, Gansu, Shanxi Province, and so on (Figure 1) [27]. The area, population, and GDP (Gross Domestic Product) of the basin approximately account for 15%, 34%, and 38% of the national totals, respectively [28]. The basin includes the primary centers of politics, economy, and culture of China. In the eastern part, the plain is the agricultural production pole of China. The predominance of various climates (from arid to humid climate) leads to the uneven precipitation distribution. The average annual evaporation and precipitation are 1699.5 mm and 556.0 mm, respectively [29], about 60–80% of the precipitation falling in the rainy season (from June to October). The average annual precipitation from 1960 to 2010 of the three first-level river basins (the Yellow River Basin, Huai River Basin, and Hai River Basin) were 439.9 mm, 854.2 mm, and 538.1 mm, respectively [30]. The maximum precipitation can be more than 2000 mm in the southeast coastal areas, while the minimum precipitation can be below 400 mm in the northwest arid regions [31]. The precipitation in the southeastern part of the Yellow River Basin is more than that in the northwest region, and the precipitation in the mountainous of the Huai River Basin is more than that in the plain area, while the precipitation in the Hai River Basin shows the opposite distribution trend with the Huai River Basin. [32]. The abundant vegetation—including alpine meadow, bushes, and farmland vegetation—can be divided into natural (45.7%) and artificial (53.0%) vegetation [33]. Natural vegetation and rain-fed agriculture are relying on precipitation, so climate components (precipitation and temperature) have significant roles to play. Irrigated agriculture vegetation depends mainly on irrigation water, so human activities have principal influence on it. Recently, droughts and floods have happened more frequently in the basin, which have aggravated the water and environmental issues, which are related to vegetation. Therefore, studies in vegetation growth response towards precipitation patterns in this basin are essential to offer a reference for vegetation conservation and water resource management.

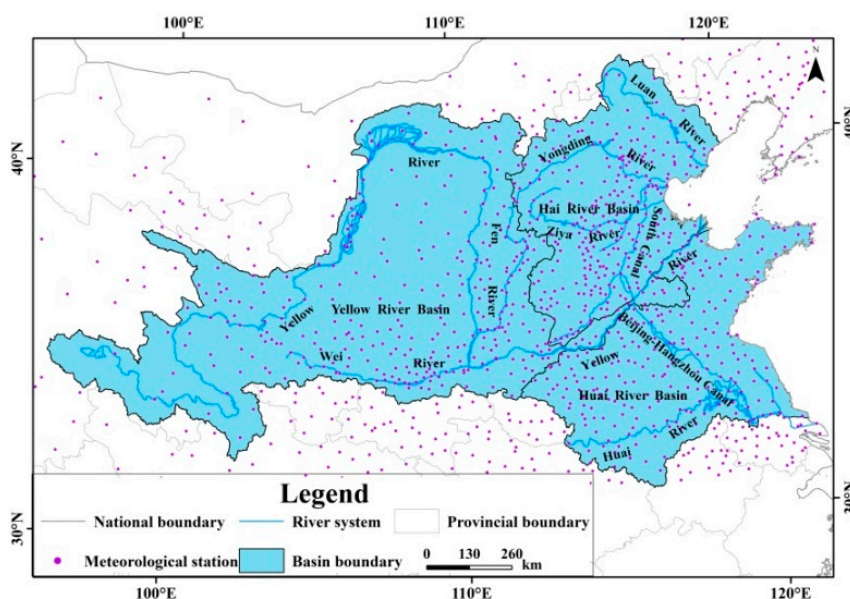


Figure 1. The Huang-Huai-Hai River Basin.

2.2. Data Sources and Processing

NDVI data were derived from the National Aeronautics and Space Administration (NASA) [34]. GIMMS NDVI data—with a temporal resolution of 15 days and a spatial resolution of 8 km (from 1982 to 2006)—were acquired from NOAA (National Oceanic and Atmospheric Administration) using the AVHRR (Advanced Very High Resolution Radiometer) method. MODIS (Moderate Resolution Imaging Spectroradiometer) NDVI data—with a temporal resolution of one month and a spatial resolution of 1 km (from 2000 to 2011)—were extracted from the MOD13A3 (Global MOD13A3 data are provided monthly at 1-kilometer spatial resolution as a gridded level-3 product in the Sinusoidal projection) dataset. For exploring the most recent vegetation activities, GIMMS NDVI data between 2007 and 2011 have to be obtained. In this case, MODIS NDVI data seems the best choice for complementing GIMMS NDVI data [35]. As these data do not come from the same kind of sensor, preliminary processing and consistency checking are needed before combined utilization [36,37]. The MVC (Maximum Value Composition) method was used to eliminate the influence from different temporal resolutions. GIMMS NDVI output data have a temporal resolution of one month [37]. The resampling method was used to obtain MODIS NDVI data with a spatial resolution of 8 km. The relationship established between both kinds of NDVI from 2000 to 2006 shows a correlation coefficient of 95%. Using the pixel regression method, we obtained GIMMS NDVI data from 2007 to 2011 from the MODIS NDVI data. During the growing season, NDVI acquisitions are not disrupted by inter-annual snow, sand, and dust [38]. Moreover, vegetation coverage development occurs mainly during that time [39–41]. Thus, this is the only period considered in this study. Equation (1) calculates vegetation coverage [42]:

$$fc = (\text{NDVI} - \text{NDVI}_{\text{soil}}) / (\text{NDVI}_{\text{veg}} - \text{NDVI}_{\text{soil}}) \quad (1)$$

where fc is the vegetation coverage of each pixel, $\text{NDVI}_{\text{soil}}$ is the NDVI of the pixel with no vegetation cover, and NDVI_{veg} is the NDVI of the pixel with full vegetation cover.

Precipitation data were extracted from China's Ground Precipitation $0.5^\circ \times 0.5^\circ$ gridded dataset (V3.0) established by the Meteorological Records Office of the National Meteorological Information Center of China [43]. The 1109 stations selected as study stations have continuous observational precipitation data (from 1982 to 2011) and are located inside or nearby the basin (Figure 1). The vector diagram was computed by the ArcGIS10.2.2 software platform (Redlands, CA, USA, Environmental Systems Research Institute) from precipitation data, and interpolated by the IDW (Inversed Distance Weighted) method [44]. At the end, the grid figure obtained has a spatial resolution of 5 km, including daily precipitation information. Rainless (daily precipitation below 5 mm) and rainstorm days (daily precipitation is above 50 mm) grid figures are also obtained.

2.3. Time Series Analysis

Trend line analysis can simulate the trend of each grid [45] and reflect the characteristics of spatial variation. One variable linear regression method allowed the analysis of the trend of the vegetation cover change, precipitation, and precipitation anomalies. Equation (2) calculates the slope of the linear time trend of each pixel by ArcGIS10.2.2 software (Redlands, CA, USA, Environmental Systems Research Institute):

$$\text{Slope} = \frac{n \times \sum_{i=1}^n (i \times K_i) - \sum_{i=1}^n i \times \sum_{i=1}^n K_i}{n \times \sum_{i=1}^n i^2 - (\sum_{i=1}^n i)^2} \quad (2)$$

where n is the cumulative number of monitoring years. In this study n is 30, and i is the year taken into account (1 refers to 1982, 2 to 1983, and so on). K_i is the value in year i (K can be the value of the NDVI, the precipitation, the rainless days, and the rainstorm days). *Slope*, the slope of the linear time trend for each pixel, is the average annual rate of vegetation cover, precipitation, rainless days, and

rainstorm days from 1982 to 2011. When the *Slope* is above 0, the trend from 1982 to 2011 is increasing, and vice versa.

The Mann-Kendall nonparametric statistical tests method—recommended by the World Meteorological Organization (WMO) [46]—was used to explore the confidence level of the change trend of vegetation coverage, precipitation, rainless days, and rainstorm days. Compared to the parametric test method, the MK nonparametric statistical tests method is more suitable for calculating the hydrology-metrological time trend, which is not influenced by outliers and involves a simple calculation process [47]. The calculation process shown in Equation (3) calculates the standardized statistic M of the time series value R_l ($l = 1982, \dots, 2011$) in each grid:

$$M = \tau / \delta, \tau = \frac{4S}{N(N-1)} - 1, \delta^2 = \frac{2(2N+5)}{9N(N-1)} \quad (3)$$

where τ is the Kendall statistical magnitude; δ^2 is variance. S is the number of occurrences of $R_{l_1} < R_{l_2}$ in all allelomorphs of the time series. ($R_{l_1}, R_{l_2}, 1982 \leq l_1 \leq l_2 \leq 2011$) of R_l (R_l is the time series value of each grid in some year, use l to represent the year, $l = 1982, \dots, 2011$; l_1 and l_2 are some two years from 1982 to 2011, $1982 \leq l_1 \leq l_2 \leq 2011$; the time series value can be the value of the NDVI, the precipitation, the rainless days, and the rainstorm days); N is 30. M is the standardized statistic, which obeys the standard normal distribution. If M is positive, it indicates an increasing trend, and vice versa. When $p = 0.05$, if the time series has a significant change trend, then the $|M| > Ma = 1.645$, indicating that the time series have passed the significance testing of 95%.

Correlation analysis is commonly used to analyze the relationship between inter-annual vegetation coverage change and climatic factors [48]. We used the Pearson linear correlation coefficient method (Equation (4)) to calculate the relationship of vegetation coverage with precipitation, rainless days, and rainstorm days:

$$r = \frac{\sum_{i=1}^n (x_i - \bar{x})(y_i - \bar{y})}{\sqrt{\sum_{i=1}^n (x_i - \bar{x})^2 \sum_{i=1}^n (y_i - \bar{y})^2}} \quad (4)$$

where x_i and y_i are the actual values of each precipitation element and vegetation coverage in every grid, respectively; \bar{x} and \bar{y} are average values of each precipitation element and vegetation coverage in every grid, respectively; i is the serial number of the year, i is 1 for 1982, 2 for 1983, and so on; r is the correlation coefficient of x and y in each grid.

2.4. Spatial Clustering Analysis

Based on the grid graph of the normalized tendency rate of vegetation coverage, precipitation, rainless days, and rainstorm days, we used the ArcGIS Spatial Analyst Tools (ArcGIS10.2.2, Redlands, CA, USA, Environmental Systems Research Institute) to cluster the grid graphs mentioned above by the Euclidean shortest distance clustering method. In order to eliminate the influence of irrigation water, we have removed the large-scale irrigated districts before clustering.

3. Results and Discussion

3.1. Spatio-Temporal Patterns of Precipitation

3.1.1. Spatial Patterns of Precipitation

The distribution of precipitation is declining from the southeast coast to the northwest inland (Figure 2a). The mean annual precipitation from 1982 to 2011 of the whole basin was 486.0 mm, and regional minimum precipitation was 119.1 mm, which happened in the Yellow River Basin, while the maximum precipitation was 1099.5 mm, which was 9.2 times the minimum value, occurring in the

Huai River Basin. The average precipitation of the Yellow River Basin, Huai River Basin, and Hai River Basin were 470.7 mm, 399.8 mm, and 710.5 mm, respectively.

3.1.2. Spatio-Temporal Variations of Precipitation

Precipitation in about 44.7% of the areas of the whole basin has increased, while in 55.3% areas showed a decreasing trend (Figure 2b). The tendency rate of the precipitation in the whole basin, the Yellow River Basin, Huai River Basin, and Hai River Basin, were 0.6 mm/decade, -9.7 mm/decade, 16.6 mm/decade, and -16.1 mm/decade, respectively. Only in the Huai River Basin did the precipitation present an increasing trend. Precipitation in 77.1% of areas of the Yellow River Basin and 76.3% of the areas of the Hai River Basin showed a decreasing trend, in 69.9% of the areas of the Huai River Basin showed an increasing trend. The decreased areas of precipitation were primarily distributed in Gansu Province, Sichuan Province, Beijing, Tianjin, the border areas of Anhui and Hubei Provinces, and the coastal areas of Jiangsu Province. The significantly increased ($p < 0.5$) areas of precipitation were primarily distributed in the middle part of the Yellow River Basin, most areas of Qinghai Province, Shandong Province, and the downstream areas of the Huai River.

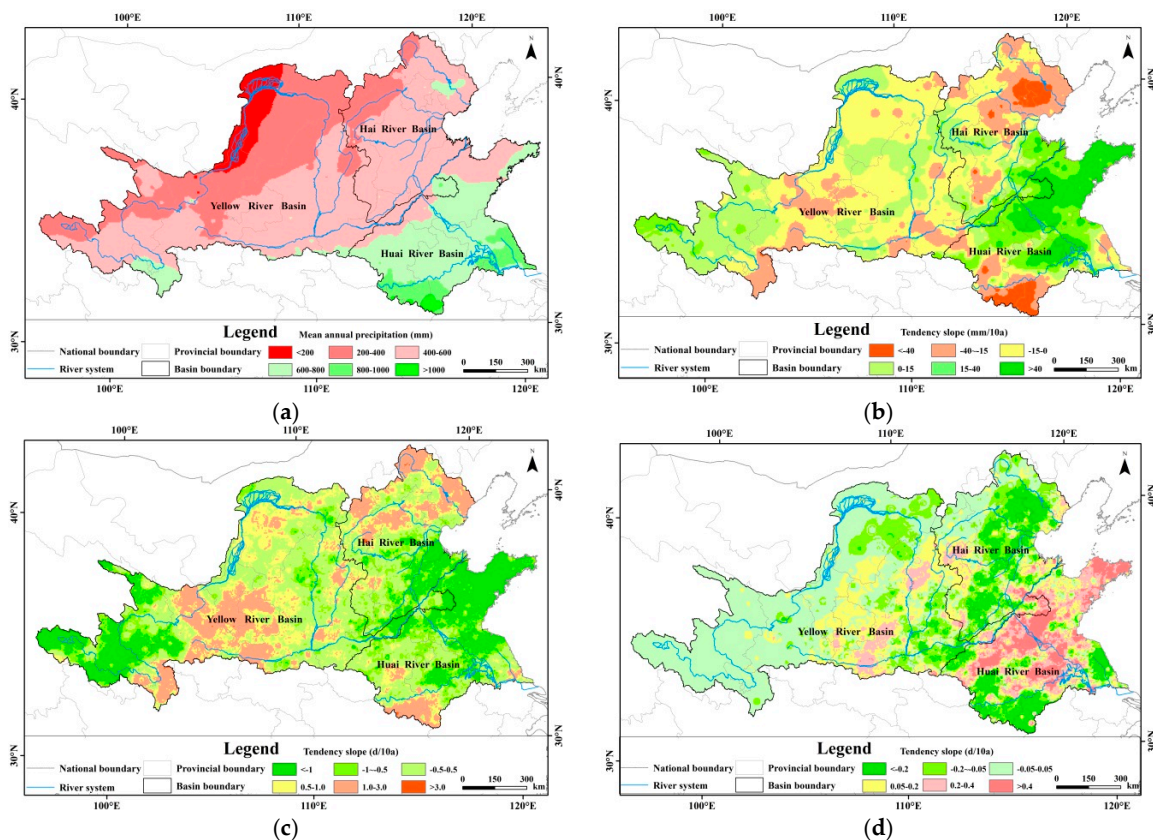


Figure 2. The spatial pattern of the mean precipitation (a), precipitation change tendency (b), rainless days change tendency (c) and rainstorm days change tendency (d) in the Huang-Huai-Hai River Basin during 1982–2011.

3.1.3. Spatio-Temporal Variations of Precipitation Anomalies

Increasing rainless days will bring about drought risk, which is detrimental to vegetation growth, so it is essential to explore the spatio-temporal variation of rainless days (Figure 2c). When compared with Figure 2b, we can find that 65.2% of the increasing areas of rainless days are nearly overlapped with the decreasing areas of precipitation, and the increasing rate of most areas were between 0.5 and 2 d/decade, and few upstream areas of the Luan River have passed the significance test ($p < 0.05$). The

decreasing areas with the rate less than -1 d/decade were mainly distributed on Tibetan Plateau, the south areas of the Hai River Basin, and most areas of the Huai River Basin, yet most areas have passed the significance test ($p < 0.05$).

The moisture brought about by rainstorms can nourish vegetation, but the rainstorm erosivity is disastrous to vegetation. To make it clear what influences rainstorms have on vegetation, we have explored the spatial distribution of the rainstorm days (Figure 2d). Rainstorm days in 43.5% of the areas of the basin presented increasing trends with the increasing rate over 0.2 d/decade, mainly distributed in the core areas of the Yellow River Basin, the west areas of the Hai River Basin and most areas of the Huai River Basin. Most areas in the Yellow River Basin and Hai River Basin have passed the significance test ($p < 0.05$), but the increasing trend in the Huai River Basin was not significant.

3.2. Spatio-Temporal Patterns of Vegetation Coverage

3.2.1. Spatial Patterns of NDVI

The NDVI presents the same variation tendency with precipitation, which is declining from the southeast coast to the northwest inland with an average NDVI of 0.42, indicating that the vegetation condition has a close relationship with precipitation (Figure 3a). The vegetation is denser in the Huai River Basin with an average NDVI of 0.51, and in the Hai River Basin with a middle-average NDVI of 0.48. However, in the Yellow River Basin, the average NDVI is much lower (0.36). Poor vegetation may be due to the long-term low precipitation on the Loess Plateau. In that way, the vegetation could not obtain sufficient moisture for a long time, leading to a barren cover. However, the Tibetan Plateau has a lush greenery which may be due to the presence of precipitation in the area [49].

3.2.2. Spatio-Temporal Variations of Vegetation Coverage

NDVI spatial distribution, which reflects the overall trend, does not reveal significant variations of vegetation coverage. The trend line analysis method, used to simulate the trend for each grid, can reflect the spatial characteristics of vegetation coverage. Figure 3b illustrates the spatial distribution of vegetation coverage change tendency from 1982 to 2011, which is consistent with previous studies [50]. The vegetation coverage has been improved with a rate above 0.01/decade in 35.6% of the basin. However the greenery was scattered in other parts (29.6%) with the rate below -0.01 /decade. In the rest of the regions (34.8%) there has been no obvious change with the rate between -0.01 /decade and 0.01/decade. There is a slight increase throughout the basin. The improved regions were located at the border areas of Inner Mongolia, and Shanxi and Shaanxi Provinces, which belong to the regions of the Three North Shelterbelt Program (these results are confirmed by Wang et al. [51]). In the upstream regions of the Yongding River, the border areas of Hebei and Shandong Provinces, and the areas along the Huai River, the improving rate was about 0.05/decade ($p < 0.05$). It is worth noting that the vegetation condition in the source regions of the Yellow River located on the Tibetan Plateau presents an improving tendency, where human activities are rare; this may be caused by climate change. The degraded regions were located at the areas along the Wei River and Fen River, the core areas of Shaanxi Province, the border areas of Shaanxi and Gansu Provinces, the areas along the Yellow River, which belong to the Hai River Basin, the areas along the Ziya River, the Beijing-Tianjin areas, the coastal areas of Shandong Province, and the northern areas of Jiangsu Province, with a decreasing rate of -0.05 /decade, but the degradation was not significant. All in all, the degraded regions are mainly located in the areas with dense population where human activities are frequent and the areas with dry climate where water resources are deficient, indicating that vegetation degradation has a close relationship with human activities and moisture.

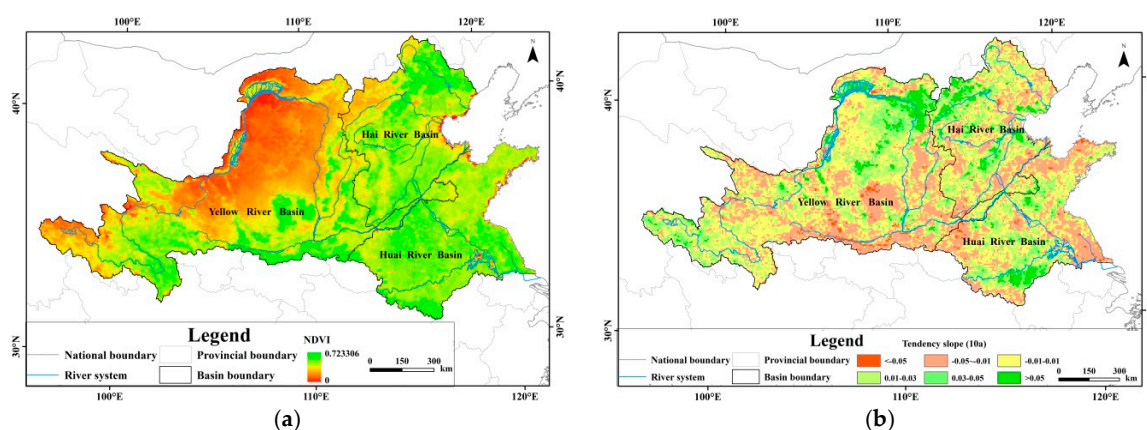


Figure 3. The spatial pattern of mean NDVI (a) and the vegetation coverage change tendency (b) in the Huang-Huai-Hai River Basin during 1982–2011.

3.3. Correlation of Vegetation Coverage and Precipitation

3.3.1. The Relationship between Vegetation Coverage and Precipitation

The relationship between vegetation coverage and precipitation is positive (Figure 5a). The area percentage of the regions where vegetation coverage showed a positive correlation with precipitation was 61.6%. The maximum coefficient was 0.8, most of them varied from 0.1 to 0.6. Regions with a positive correlation were mainly distributed in the north areas. Most of the regions were located at arid and semiarid areas, with low precipitation and high evaporation, so the soil is dry and surface water resources are insufficient. Precipitation is the main source of local vegetation growth, so the vegetation has a high reliance on precipitation, leading to a positive correlation. Regions with a negative correlation were mainly distributed in the northern coastal areas and midstream areas of the Ziya River and most areas of the Huai River Basin, where population density is high and human activities are frequent. In these areas, though the precipitation has increased, the vegetation has not improved, illustrating that human activities have an adverse impact on vegetation (because human activities are beyond our research, we will not explain them). At the same time, part of the irrigation districts (including the Wei River Irrigation District and the North China Plain Irrigation Districts), the areas with dense river networks and the source areas of the Yellow River presented low correlations. The reason for the low correlations in irrigation districts and dense river network areas could be the abundant surface water in these areas which can supply sufficient moisture for vegetation, leading to less dependence on precipitation. Additionally, the low correlation in the source areas of the Yellow River may be due to the snow melt water which can supply moisture to vegetation growth. The result is coincident with the study by Shen and Zhou [52].

To have a deeper understanding about the impact of precipitation on vegetation, we have also studied the relationship between inter-annual NDVI and precipitation. Due to the large span of the Huang-Huai-Hai River Basin, precipitation and NDVI in different first-level river basins were variable, so we have explored each basin, respectively. The response relationship of NDVI and precipitation in the whole basin and the three first-level river basins are all in good condition, especially in 1989, 1999, 2006, and 2009 (Figure 4). From the inter-annual variations, we can divide the 30 years into four phases: (1) a slowly increasing phase (from 1982 to 1985); in this phase, NDVI in different basins was increasing with high precipitation, but the increasing range was not obvious; (2) a large fluctuations phase (from 1986 to 1998); in this phase, NDVI in different basins fluctuated corresponding with the sharp fluctuations of precipitation; (3) a slowly decreasing phase (from 1999 to 2002); in this phase, NDVI was gradually reducing with the low precipitation; and (4) an increasing phase (from 2003 to 2011); in this phase, NDVI started to continue increasing after the high precipitation in 2003, but NDVI

has not presented a sharp rise corresponding to the large increase of precipitation in 2003. Instead it increased sharply in 2004, which could be due to the low precipitation in 2002, when the soil was dry. In order to replenish the shortage of soil water, less precipitation can nourish the vegetation, resulting in the vegetation lag to precipitation, which is coincident with others research [53,54].

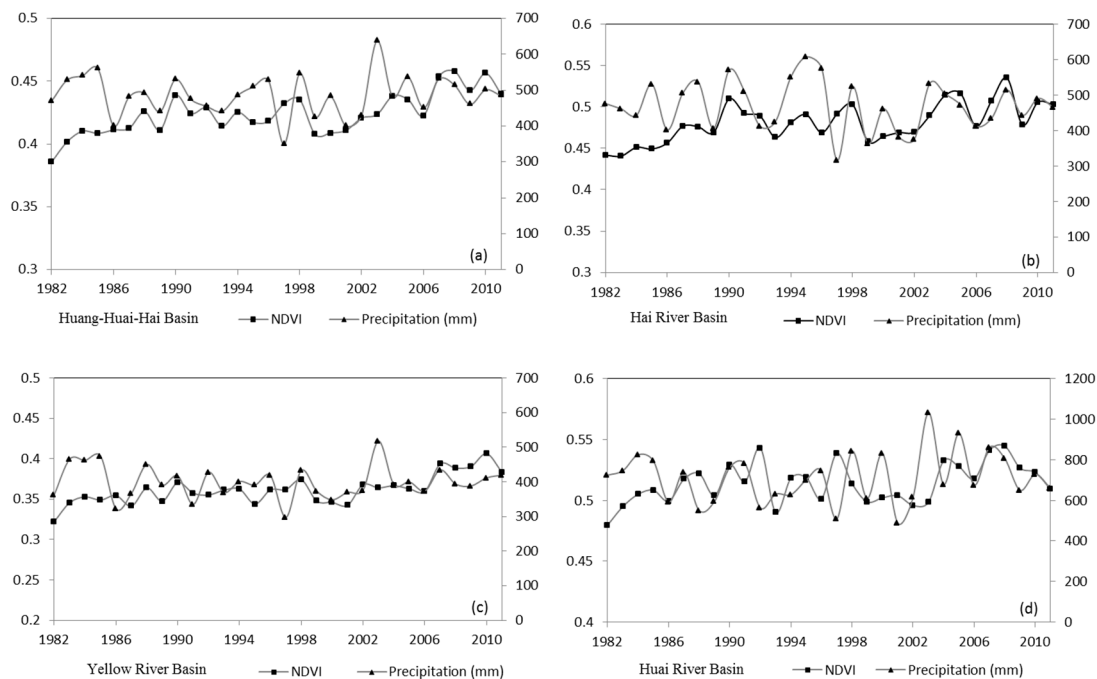


Figure 4. The inter-annual relationship between NDVI and precipitation in the Huang-Huai-Hai River Basin ((a) is for the Huang-Huai-Hai River Basin, (b) is for the Hai River Basin, (c) is for the Yellow River Basin, and (d) is for the Huai River Basin).

3.3.2. The Relationship between Vegetation Coverage and Precipitation Anomalies

Comparing the correlations between vegetation coverage and precipitation and rainless days, we find that the distribution of the relationship between vegetation coverage and rainless days is similar to the relationship between vegetation coverage and precipitation (Figure 5a,b). Most areas with negative correlation were overlapped with the positive correlation areas of precipitation, mainly distributed in the arid and semi-arid regions in the northern part. In the whole basin, the relationship between vegetation coverage and rainless days is negative. The area percentage of the regions where vegetation coverage showed a negative correlation with rainless days was 62.7%. The minimum coefficient was -0.8 , most of them varied from -0.6 to -0.1 . It is observed from Figure 2c that the rainless days in these areas have increased, indicating that drought risk in these areas has enhanced, which has a detrimental impact on vegetation. Positive correlation areas are mainly distributed in a few areas of the Tibetan Plateau, the core areas in the Hai River Basin, and most areas of the Huai River Basin. From Figures 2c and 3b we can observe that most of the areas, including the areas in the Tibetan Plateau, the areas in the Hai River Basin, and the valley areas of the Huai River, presented increasing rainless days coupled with improving vegetation cover. The reason for this result may be related to the local ecological recovery. Most areas in the Huai River Basin showed decreasing rainless days coupled with degrading vegetation cover, indicating that the decreasing of rainless days has not resulted in vegetation improvement, though the vegetation degradation may be influenced by other factors.

In the whole basin, the correlation between vegetation coverage and rainstorm days is low, and the correlation coefficient in most areas was between -0.3 and 0.3 (Figure 5c). Around the whole basin, the relationship between vegetation coverage and rainless days is negative. The area percentage of the

regions where vegetation coverage showed a negative correlation with precipitation was 60.3%. The minimum coefficient was -0.8 , most of them varied from -0.6 to 0 . It is worth noting that some parts of the Yellow River Basin, Huai River Basin, and Beijing-Tianjin presented positive correlations with coefficients between 0.3 and 0.6 . From Figures 2d and 3b, we can know that the rainstorm days and vegetation coverage have both decreased in the Beijing-Tianjin region, illustrating that the reduction of rainstorm days has not brought about beneficial effects upon vegetation, and vegetation degradation may be caused by frequent human activities. While the other positive areas with rainstorm days and vegetation coverage have both increased, this may be the increasing rainstorm days that have supplied the moisture for the vegetation growth and prompted the vegetation condition. This could be due to the implementation of the Three North Shelter Forest and other ecological restoration projects that have prompted the vegetation improvement [51,52]. Since human activities are beyond our research, we will not explain them. Most areas of the Huai River Basin presented negative correlations, and the increasing rainstorm days have brought about an adverse impact on the vegetation, resulting in the vegetation degradation in these areas.

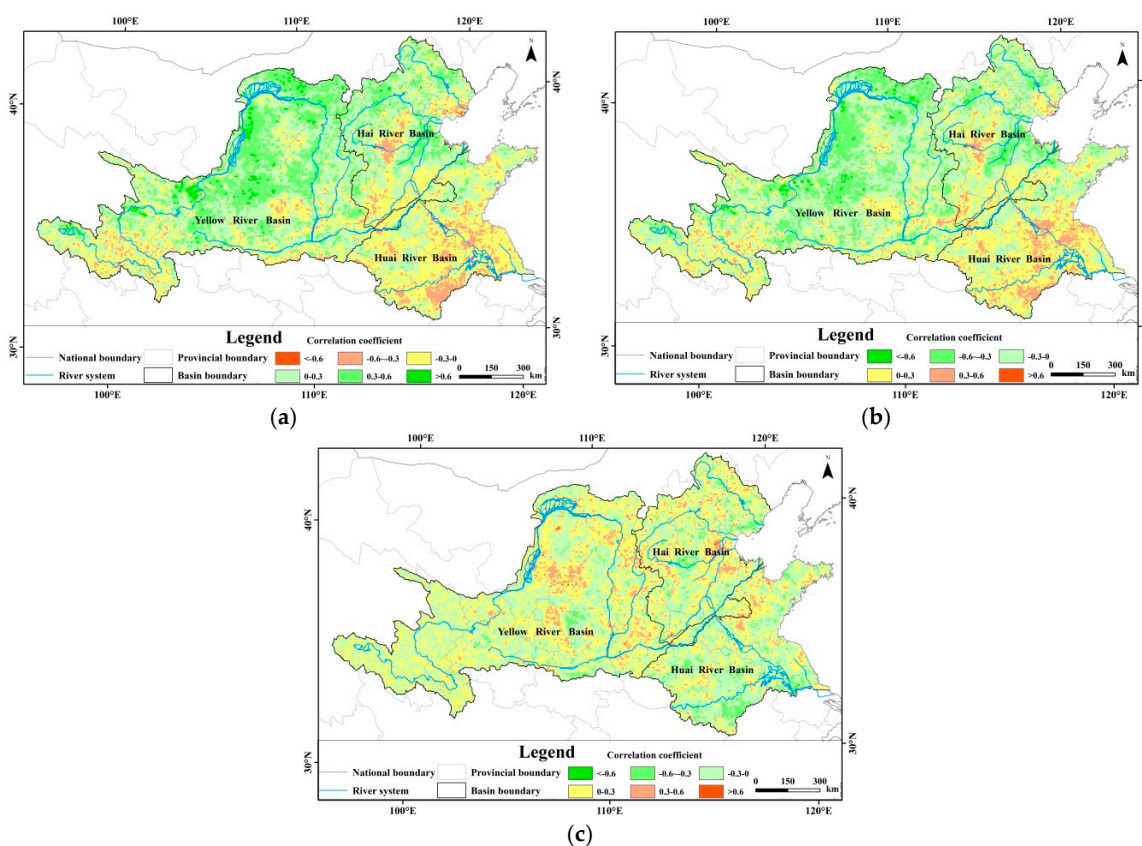


Figure 5. The correlations between vegetation coverage and precipitation factors in the Huang-Huai-Hai River Basin during 1982–2011 ((a) with precipitation; (b) with rainless days; (c) with rainstorm days).

3.4. Multi-Factor Cluster Analysis

Vegetation cover degraded by decreasing precipitation and increasing precipitation anomalies was mainly distributed in most areas of the Yellow River Basin and the northern and western Huai River Basin (Figure 6). These areas belong to arid and semi-arid regions with vulnerable ecosystems, where the vegetation growth is highly dependent on precipitation. Thus, the precipitation anomalies have strong influence on vegetation. However, in most areas of Shandong Province, vegetation has degraded due to the condition of increasing precipitation and increasing rainstorm days, indicating that extreme events have an adverse effect on vegetation growth. The areas with

degrading vegetation on the condition of decreasing precipitation and increasing rainless days were mainly located in the Beijing-Tianjin region, and the areas with improving vegetation on the condition of increasing precipitation and decreasing rainless days were mainly distributed in the Tibetan Plateau. The phenomenon indicates that the precipitation has a close relationship with vegetation cover. In addition, there are some special regions with improving vegetation on the condition of decreasing precipitation and increasing precipitation anomalies. These regions were mainly distributed in the Three North Shelterbelt, Tibetan Plateau, and some regions along the rivers. The improvement in vegetation in the Three North Shelterbelt region may be due to the ecological construction [51]. Li et al. also found the ecological restorations to be the primary driving factors for vegetation improvement in these areas [55]. In Tibetan Plateau, the snow melting water resulting from climate change, has supplied enough moisture to the growth of vegetation [56]. The vegetation cover improvement in the river areas may be due to the water from the river which can nourish the vegetation and some ecological constructions implemented along these rivers have brought about vegetation improvement [51,52].

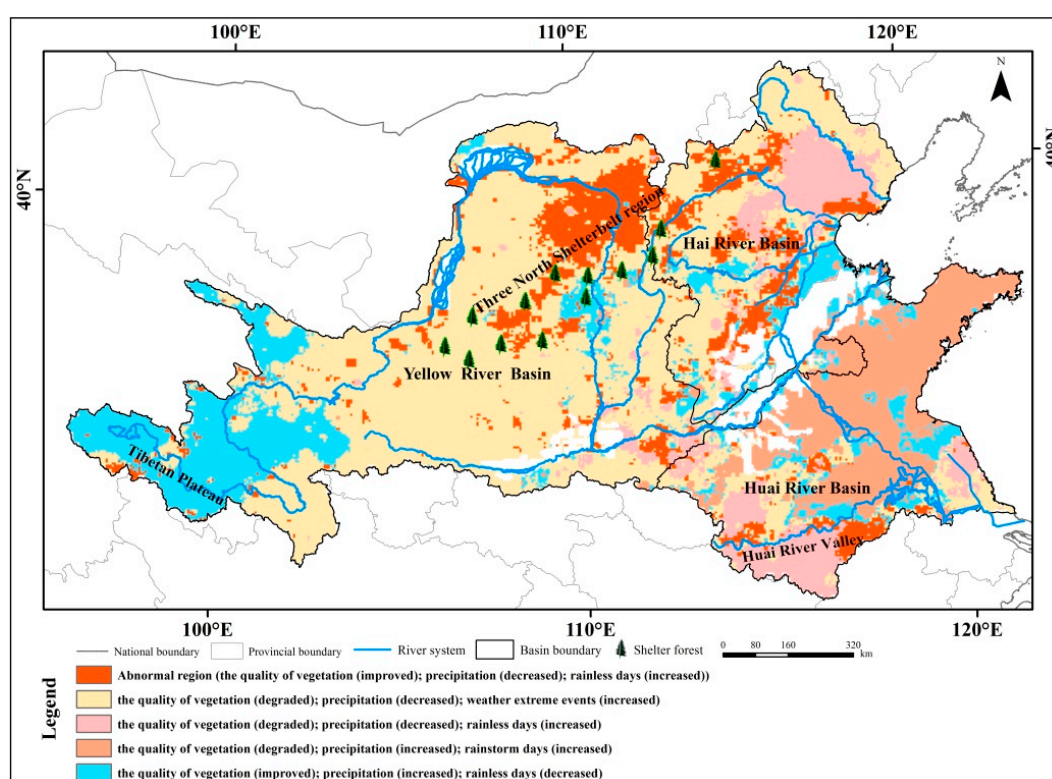


Figure 6. The coupling relationship between vegetation coverage and precipitation factors in the Huang-Huai-Hai River Basin.

4. Conclusions

Understanding the relationship between precipitation, precipitation anomalies and vegetation activity are necessary to estimate the potential impacts of precipitation on vegetation, especially in arid regions and densely-populated areas. The quantitative analyses presented in this study have illustrated the relationship between precipitation factors and vegetation. The spatial distributions of average precipitation and average NDVI are quite similar. They are all declining from the southeast coast to the northwest inland, indicating that the distribution of NDVI is influenced by precipitation. The scattered vegetation was mainly located in densely populated areas where human activities are frequent, and dry climate areas where water resources are scarce. Thus, vegetation degradation should be connected with human activities and moisture. The correlation between vegetation coverage and

precipitation changes was positive, and the response relationships of annual NDVI and precipitation in the whole basin and the three first-level river basins were all very good, indicating that precipitation was the important factor of vegetation growth. Precipitation anomalies (including rainless days and rainstorm days) have adverse influence on vegetation growth, especially in arid and semi-arid regions. Since surface water is very scarce in arid and semi-arid regions, precipitation is the main moisture source of local vegetation growth, as vegetation has a high dependence on precipitation.

The clustering result shows that vegetation coverage change was caused by both meteorological factors and human activities in the Huang-Huai-Hai River Basin. The degradation of vegetation in the Huai River Basin was mainly caused by increasing precipitation anomalies, and in the Yellow River Basin and Hai River Basin, the decreasing precipitation and increasing precipitation anomalies were both important factors for vegetation degradation. The results presented in this study have illustrated the influences on vegetation of precipitation anomalies for wide areas of the Huang-Huai-Hai River Basin. These results can provide references for the research on the impact of disasters on vegetation ecosystem. The regions with increasing precipitation anomalies will be more prone to extreme events like droughts and floods. In these regions, important ecosystem services supplied by vegetation ecosystem, such as raw material production, erosion regulation, climate regulation, and so on, can be seriously affected by precipitation anomalies. In order to have a comprehensive understanding of the vegetation variations and make prediction for vegetation anomalies, it is necessary to conduct the prediction research on precipitation anomalies in the future. Furthermore, the results can support opinions for government to conduct land cover use plan appropriately.

From the clustering result, we find that the ecological constructions were also significant factors influencing vegetation improvement. These results will enrich our knowledge about the influence of ecological restoration projects on vegetation activity in the basin, especially in the Three North Shelterbelt. Though the vegetation has improved in these regions, the area in western and northern of China is still in preliminary recovery with weak self-regulation capability, poor stability. It is difficult to form steady ecological system in a short period [57]. More efforts should be made to promote the implementation of ecological recovery project, and strengthen the continuous monitoring of vegetation activity dynamic.

In this paper, we have explored the influence from precipitation and precipitation anomalies on vegetation. The result could help to deliver some recommendations on vegetation recovery for relevant departments and other researchers. There are also some other factors affecting vegetation. In order to conduct a comprehensive investigation of the vegetation variations, the following research should consider more factors, such as human activities, temperature, and so on.

Acknowledgments: We are grateful to the National Meteorological Information Center of China and NASA to share the meteorological data and NDVI data. We also thank the editors and anonymous reviewers. This work was supported by the National Key Research and Development Project (No. 2016YFA0601503) and the Representative Achievements and Cultivation Project of State Key Laboratory of Simulation and Regulation of Water Cycle in River Basin (No. 2016CG02).

Author Contributions: Denghua Yan designed the project and provided overall guidance. Ting Xu drafted the manuscript. Denghua Yan, Ting Xu, Abel Girma, and Pierre Do finalized the manuscript. Zhe Yuan, Baisha Weng, Tianling Qin, and Yong Yuan collected and calculated the data. All authors reviewed the manuscript.

Conflicts of Interest: The authors declare no conflict of interest in any aspect of the data collection, analysis or the preparation of this paper.

References

1. Cramer, W.P.; Leemans, R. *Assessing Impacts of Climate Change on Vegetation Using Climate Classification Systems in Vegetation Dynamics & Global Change*; Springer: New York, NY, USA, 1993; pp. 190–217.
2. Myneni, R.B.; Keeling, C.D.; Tucker, C.J.; Asrar, G.; Nemani, R.R. Increased Plant Growth in the Northern High Latitudes from 1981 to 1991. *Nature* **1997**, *386*, 698–702. [[CrossRef](#)]
3. Liu, Z.; Feng, M.; Zhou, W.; Li, Q. Research the dynamics of landscape spatial pattern of urban-rural ecotone using multi-temporal remote sensing image. *IEEE Geosci. Remote Sens. Symp.* **2009**, *5*, 264–267.

4. Karlson, M.; Ostwald, M. Remote sensing of vegetation in the Sudano-Sahelian zone: A literature review from 1975 to 2014. *J. Arid Environ.* **2016**, *124*, 257–269. [[CrossRef](#)]
5. Feng, T.; Martin, B.; Liu, Y.Y.; Aleixandre, V.; Torbern, T.; Abdoul, A.D.; Kjeld, R.; Cheikh, M.; Wang, Y.J.; Rasmus, F. Remote sensing of vegetation dynamics in drylands: Evaluating vegetation optical depth (VOD) using AVHRR NDVI and in situ, green biomass data over West African Sahel. *Remote Sens. Environ.* **2016**, *177*, 265–276.
6. Slayback, D.A.; Pinzon, J.E.; Los, S.O.; Tucker, C.J. Northern hemisphere photosynthetic trends 1982–1999. *Glob. Chang. Biol.* **2013**, *9*, 1–15. [[CrossRef](#)]
7. Alcaraz-Segura, D.; Liras, E.; Tabik, S.; Paruelo, J.; Cabello, J. Evaluating the consistency of the 1982–1999 NDVI trends in the Iberian Peninsula across four time-series derived from the AVHRR sensor: LTDR, GIMMS, FASIR, and PAL-II. *Sensors* **2010**, *10*, 1291–1314. [[CrossRef](#)] [[PubMed](#)]
8. Beck, P.S.A.; Goetz, S.J. Satellite observations of high northern latitude vegetation productivity changes between 1982 and 2008: Ecological variability and regional differences. *Environ. Res. Lett.* **2011**, *6*, 5501–5511. [[CrossRef](#)]
9. Gonsamo, A.; Chen, J.M. Circumpolar vegetation dynamics product for global change study. *Remote Sens. Environ.* **2016**, *182*, 13–26. [[CrossRef](#)]
10. Gao, Q.Z.; Guo, Y.Q.; Xu, H.M.; Hasbagen, G.; Li, Y.; Wan, Y.F.; Qin, X.B.; Ma, X.; Liu, S. Climate change and its impacts on vegetation distribution and net primary productivity of the alpine ecosystem in the Qinghai-Tibetan Plateau. *Sci. Total Environ.* **2016**, *554–555*, 34–41. [[CrossRef](#)] [[PubMed](#)]
11. Rodrigues, J.M.; Behling, H.; Giesecke, T. Holocene dynamics of vegetation change in southern and southeastern Brazil is consistent with climate forcing. *Quat. Sci. Rev.* **2016**, *146*, 54–65. [[CrossRef](#)]
12. Intergovernmental Panel on Climate Change(IPCC). Climate Change 2007. In *The Physical Science Basis*; Cambridge University Press: Cambridge, UK, 2007.
13. Benhadj, I.; Simonneaux, V.; Mougnot, B.; Khabba, S.; Chehbouni, A. Land Use and Crop Evapotranspiration in Tensift/Marrakech Plain: Inter-Annual Analysis Based on MODIS Satellite Data. In Proceedings of the 13th IWRA World Water Congress, Montpellier, France, 1–4 September 2008; pp. 1–15.
14. Spano, D.; Cesaraccio, C.; Duce, P.; Snyder, R.L. Phenological stages of natural species and their use as climate indicators. *Int. Biometeorol.* **1999**, *42*, 124–133. [[CrossRef](#)]
15. Li, J.; Lewis, J.; Rowland, J.; Tappan, G.; Tieszen, L.L. Evaluation of land performance in Senegal using multi-temporal NDVI and rainfall series. *J. Arid Environ.* **2004**, *59*, 463–480. [[CrossRef](#)]
16. Wessels, K.J.; Prince, S.D.; Malherbe, J.; Smallc, J.; Frostd, P.E.; van Zyl, D. Can human-induced land degradation be distinguished from the effects of rainfall variability? A case study in South Africa. *J. Arid Environ.* **2007**, *68*, 271–297.
17. Li, A.; Wu, J.; Huang, J. Distinguishing between human-induced and climate-driven vegetation changes: A critical application of RESTREND in inner Mongolia. *Landsc. Ecol.* **2012**, *27*, 969–982. [[CrossRef](#)]
18. Buyantuyev, A.; Wu, J. Urbanization alters spatiotemporal patterns of ecosystem primary production: A case study of the Phoenix metropolitan region USA. *J. Arid Environ.* **2009**, *73*, 512–520. [[CrossRef](#)]
19. Gessner, U.; Naeimi, V.; Klein, I.; Kuenzer, C.; Klein, D.; Dech, S. The relationship between precipitation anomalies and satellite-derived vegetation activity in Central Asia. *Glob. Planet. Chang.* **2012**, *110*, 74–87. [[CrossRef](#)]
20. Fu, B.J.; Liu, Y.; Lv, Y.; He, C.S.; Zeng, Y.; Wu, B.F. Assessing the soil erosion control service of ecosystems change in the Loess Plateau of China. *Ecol. Complex.* **2011**, *8*, 284–293. [[CrossRef](#)]
21. Liu, Q.; Yang, Z.; Cui, B. Spatial and temporal variability of annual precipitation during 1961–2006 in Yellow River Basin, China. *J. Hydrol.* **2008**, *361*, 330–338. [[CrossRef](#)]
22. Wang, W.; Shao, Q.X.; Peng, S.Z.; Zhang, Z.X.; Xing, W.Q.; An, G.Y.; Yong, B. Spatial and temporal characteristics of changes in precipitation during 1957–2007 in the Haihe River basin, China. *Stoch. Environ. Res. Risk Assess.* **2011**, *25*, 881–895. [[CrossRef](#)]
23. Sun, R.; Liu, C.M.; Zhu, Q.J. Relationship between fractional vegetation cover change and rainfall in the Yellow River Basin. *Acta Geogr. Sci.* **2001**, *56*, 667–672. (In Chinese)
24. Jing, X.; Yao, W.Q.; Wang, J.H.; Song, X.Y. A study on the relationship between dynamic change of vegetation coverage and precipitation in Beijing’s mountainous areas during the last 20 years. *Math. Comput. Model.* **2011**, *54*, 1079–1085. [[CrossRef](#)]

25. Zhao, A.Z.; Liu, X.F.; Zhu, X.F.; Pan, Y.Z.; Chen, Y.C. Spatiotemporal analyses and associated driving forces of vegetation coverage change in the Loess Plateau. *Chin. Environ. Sci.* **2016**, *36*, 1568–1578. (In Chinese)
26. Pang, G.; Wang, X.; Yang, M. Using the NDVI to identify variations in, and responses of, vegetation to climate change on the Tibetan Plateau from 1982 to 2012. *Quat. Int.* **2016**, 1–10. [[CrossRef](#)]
27. Yin, J.; Yan, D.H.; Yang, Z.Y.; Yuan, Z.; Zhang, C. Projection of extreme precipitation in the context of climate change in Huang-Huai-Hai region, China. *J. Earth Syst. Sci.* **2016**, *125*, 1–13. [[CrossRef](#)]
28. Yan, D.H.; Wu, D.; Huang, R.; Wang, L.N.; Yang, G.Y. Drought evolution characteristics and precipitation intensity changes during alternating dry-wet changes in the Huang-Huai-Hai River basin. *Hydrol. Earth Syst. Sci.* **2013**, *17*, 2859–2871. [[CrossRef](#)]
29. Guo, J.; Ren, G.Y. Recent change of pan evaporation and possible climate factors over the Huang-Huai-Hai watershed, China. *Adv. Water Sci.* **2005**, *16*, 666–672. (In Chinese)
30. Zhang, D.D.; Yan, D.H.; Wang, Y.C.; Lu, F.; Wu, D. Changes in extreme precipitation in the Huang-Huai-Hai River basin of China during 1960–2010. *Theor. Appl. Climatol.* **2015**, *120*, 195–209. [[CrossRef](#)]
31. Wang, G.Q.; Zhang, J.Y. Variation of water resources in the Huang-Huai-Hai areas and adaptive strategies to climate change. *Quat. Int.* **2015**, *380–381*, 180–186. [[CrossRef](#)]
32. Shao, W.W.; Huang, H.; Wang, J.H.; Cao, L. Analysis on the development state and problems of the water resources in the basins of Yellow River, Huaihe River and Haihe River. *J. Chin. Inst. Water Resour. Hydropower Res.* **2012**, *10*, 1–9. (In Chinese)
33. Zhao, J. The Responses to Drought and Drought-Resistant Characteristics of Nature Vegetation in Huang-Huai-Hai River Basin. Master's Thesis, Donghua University, Shanghai, China, 2015; 25p. (In Chinese)
34. Available online: <http://www.nasa.gov/> (accessed on 6 July 2013).
35. Fensholt, R.; Proud, S.R. Evaluation of earth observation based global long term vegetation trends-comparing GIMMS and MODIS global NDVI time series. *Remote Sens. Environ.* **2012**, *119*, 131–147. [[CrossRef](#)]
36. Jong, R.D.; Bruin, S.D.; Schaepman, M.; Dent, D. Quantitative mapping of global land degradation using earth observations. *Int. J. Remote Sens.* **2011**, *32*, 6823–6853. [[CrossRef](#)]
37. Mao, D.H.; Wang, Z.M.; Luo, L.; Ren, C.Y. Integrating AVHRR and MODIS data to monitor NDVI changes and their relationships with climatic parameters in Northeast China. *Int. J. Appl. Earth Obs. Geoinf.* **2012**, *18*, 528–536. [[CrossRef](#)]
38. Han, X.Z.; Li, S.M.; Zhu, X.X.; Luo, J.N. China vegetation time-space change research in 20 years. In Proceedings of the China Meteorological Society Annual Conference, Chengdu, China, 25–27 October 2006; pp. 753–759.
39. Omotosho, J.B. Long-range prediction of the onset and end of the rainy season in the west African Sahel. *Int. J. Climatol.* **1992**, *12*, 369–382. [[CrossRef](#)]
40. Prince, S.D.; Colstoun, E.B.D.; Kravitz, L.L. Evidence from rain-use efficiencies does not indicate extensive sahelian desertification. *Glob. Chang. Biol.* **1998**, *4*, 359–374. [[CrossRef](#)]
41. Wang, J.; Price, K.P.; Rich, P.M. Spatial patterns of NDVI in response to precipitation and temperature in the central Great Plains. *Int. J. Remote Sens.* **2001**, *22*, 3827–3844. [[CrossRef](#)]
42. Qi, J.; Marsett, R.C.; Moran, M.S.; Goodrich, D.C.; Heilman, P.; Kerr, Y.H.; Dedieu, G.; Chehbouni, A.; Zhang, X.X. Spatial and temporal dynamics of vegetation in the San Pedro River basin area. *Agric. For. Meteorol.* **2000**, *105*, 55–68. [[CrossRef](#)]
43. Available online: <http://cdc.cma.gov.cn/> (accessed on 1 June 2013).
44. Garcia, M.; Peters-Lidard, C.D.; Goodrich, D.C. Spatial interpolation of precipitation in a dense gauge network for monsoon storm events in the southwestern United States. *Water Resour. Res.* **2008**, *44*, 5–13. [[CrossRef](#)]
45. Stow, D.; Daeschner, S.; Hope, A.; Douglas, D.; Petersen, A.; Myneni, R.; Zhou, L.; Oechel, W. Variability of the Seasonally Integrated Normalized Difference Vegetation Index Across the North Slope of Alaska in the 1990s. *Int. J. Remote Sens.* **2003**, *24*, 1111–1117. [[CrossRef](#)]
46. Thornthwaite, C.W. An Approach toward a Rational Classification of Climate. *Geogr. Rev.* **1948**, *38*, 55–89. [[CrossRef](#)]
47. Sheng, Y.; Pilon, P.; Cavadias, G. Power of the Mann-Kendall and Spearman's rho tests for detecting monotonic trends in hydrological series. *J. Hydrol.* **2002**, *259*, 254–271.
48. Dai, S.P.; Zhang, B.; Wang, H.J.; Wang, Y.M.; Guo, L.X.; Wang, X.M.; Li, D. Vegetation cover change and the driving factors over northwest China. *J. Arid Land* **2011**, *3*, 25–33.

49. Yu, H.Y.; Xu, J.C. Effects of climate change on vegetations on Qinghai-Tibet Plateau: A review. *Chin. J. Ecol.* **2009**, *28*, 747–754. (In Chinese)
50. Chen, H.L. Variations of Vegetation Cover and Its Impact on Climate and Water Source in Huanghe-Huaihe-Haihe Zone. Ph.D. Thesis, Chinese Academy Meteorological Science, Beijing, China, 2007.
51. Wang, Q.; Zhang, B.; Zhang, Z.Q.; Zhang, X.F.; Dai, S.P. The Three-North Shelterbelt Program and Dynamic Changes in Vegetation Cover. *J. Resour. Ecol.* **2014**, *5*, 53–59.
52. Shen, X.S.; Zhou, Z.Z. On the Vegetational Remaking of Mountainous Region and Hills in the Upper and Middle Reaches of Huaihe River. *J. Mt. Sci.* **2001**, *19*, 285–288.
53. Shen, B.; Fang, S.; Li, G. Vegetation Coverage Changes and Their Response to Meteorological Variables from 2000 to 2009 in Naqu, Tibet, China. *Can. J. Remote Sens.* **2014**, *40*, 67–74. [[CrossRef](#)]
54. Guo, W.; Ni, X.N.; Jing, D.; Li, S. Spatial-temporal patterns of vegetation dynamics and their relationships to climate variations in Qinghai Lake Basin using MODIS time-series data. *J. Geogr. Sci.* **2014**, *24*, 1009–1021. [[CrossRef](#)]
55. Li, S.; Liang, W.; Fu, B.J.; Lü, Y.H.; Fu, S.Y.; Wang, S.; Su, H.M. Vegetation changes in recent large-scale ecological restoration projects and subsequent impact on water resources in China's Loess Plateau. *Sci. Total Environ.* **2016**, *569–570*, 1032–1039. [[CrossRef](#)] [[PubMed](#)]
56. Xu, W.X.; Liu, X.D. Regional Pattern of Vegetation Responses to Global Warming in the Qinghai-Tibet Plateau during Late Spring and Early Summer. *Plateau Meteorol.* **2009**, *28*, 723–730. (In Chinese)
57. *A Bulletin of Status Quo of Desertification and Sandification in China*; State Forestry Administration: Beijing, China, 2011.



© 2017 by the authors. Licensee MDPI, Basel, Switzerland. This article is an open access article distributed under the terms and conditions of the Creative Commons Attribution (CC BY) license (<http://creativecommons.org/licenses/by/4.0/>).